NANO LETTERS

2007
Vol. 7, No. 10
3165−3171

Rectified Ion Transport through Concentration Gradient in Homogeneous Silica Nanochannels

Li-Jing Cheng and L. Jay Guo*

Department of Electrical Engineering and Computer Science, The University of Michigan, Ann Arbor, Michigan 48109

Received July 20, 2007; Revised Manuscript Received August 30, 2007

ABSTRACT

We investigate the ionic rectifying effect through 4 and 20 nm thick silica nanochannels placed between two ionic solutions of different concentrations. The effect was observed when only a single side of the channel has electric double-layer overlap. The calculation based on Poisson–Nernst–Planck (PNP) theory and a simplified model suggests that the phenomenon result from the accumulation and depletion of both cations and anions in the nanochannels responding to different bias polarities. The model also elucidates that the basis of the rectifying effects in the nanofluidic devices reported to date is due to the asymmetric cation/anion ratios or equivalently built-in potentials on the two sides of the nanochannels. The study benefits the design of nanofluidic devices for attoliter-scale chemical delivery.

Transport of ions through nanoscale geometries has been widely studied due to the desire and interest to understand the activity of biological ion channels in physiological processes and the prospect of exploiting the property in biomedical and chemical applications such as molecule delivery and sensing.[1] Fabricated on solid substrates, artificial nanochannels or nanopores provide robust and controllable means for more versatile applications[2−4] and can be easily integrated with microfluidic devices. The general benefit of small channel size is the capability of handling attoliter-scale samples, resulting in minimal usage of reagent, precise quantity control, and efficient processing. In addition to these benefits, nanochannels with proper channel size and reservoir bath concentrations offer selectivity to charged ions and molecules. The charge selectivity in such devices derives from the fact that when the size of nanochannels is reduced to or smaller than the Debye length, λ_D,[5] the concentration of the counter-ions in nanochannels can be enhanced while that of co-ions is diminished due to the electrostatic interaction between ions and charged channel walls.[6] In this regime, the electric double-layers (EDLs) overlap and the ion conductance through the nanochannel is governed by the surface charge instead of the bath ion concentration in the reservoirs. Such unique properties open up the possibility to selectively deliver specific types, and controllable amounts of molecules or ions through the nanochannels by electrokinetic transport.

Nanochannels serving as chemical delivery devices are usually placed between two ionic solutions of different concentrations.[2,7] Flow of ions through the nanochannel in such circumstance was observed to occur more readily in one direction than in the other. Similar asymmetric effect has been observed in conical-shaped nanopores that have asymmetric channel geometry[8] and diodelike nanochannels with asymmetric surface charge distributions.[9,10] In this Letter, we experimentally study the asymmetric ionic flux in structurally symmetric silica nanochannels with homogeneous surface charge density but placed between the asymmetric ion concentrations. We attribute the rectifying effect to the disparate ion concentration profiles produced under the applied potentials of different polarities. As illustrated in Figure 1, voltage bias of different polarities applied across a nanochannel, along with the concentration gradient in the channel, can extend or shrink the proportion of EDL overlap in the nanochannel and, therefore, cause the asymmetric ionic conductance. Theoretical calculation by using the two-dimensional Poisson−Nernst−Planck (PNP) model agrees qualitatively with the experimental results. We also provide a simplified analysis to elucidate the common mechanism that applies to all of the ionic rectifying effects reported to date. The purpose of this work is to demonstrate and analyze one of the fundamental issues encountered in the design of nanofluidic devices.

In our experiment, two different sizes of nanochannel were studied. They are both 60 μm long and equivalently 12.5 μm wide by design and fabrication. The thicknesses of the two nanochannels, determined by the experiment, are ~19 and ~4 nm, respectively. Figure 2 shows the micro-

* Corresponding author. E-mail: guo@eecs.umich.edu. Telephone: (734) 647-7718. Address: The University of Michigan, Department of Electrical Engineering and Computer Science, 1301 Beal Avenue, Ann Arbor, MI 48109.

10.1021/nl071770c CCC: $37.00
Published on Web 09/26/2007

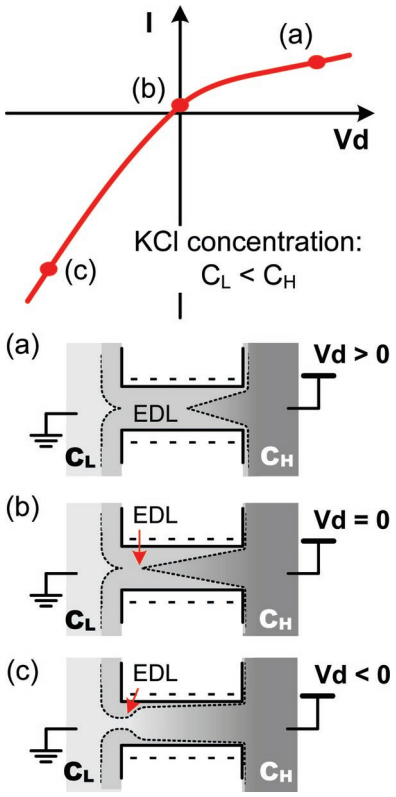

Figure 1. Rectifying effect due to the disparate ion distribution along the nanochannel having negative surface charge and under different polarities of applied potential. The gray scale plots show the relative ionic concentration in different regions of the channel. (a) High concentration C_H side is positively biased relative to the low concentration side C_L. (b) Zero bias. (c) C_H is negatively biased. The gray region within the nanochannel that is bound by the dashed lines represents the electric double layers (EDL).

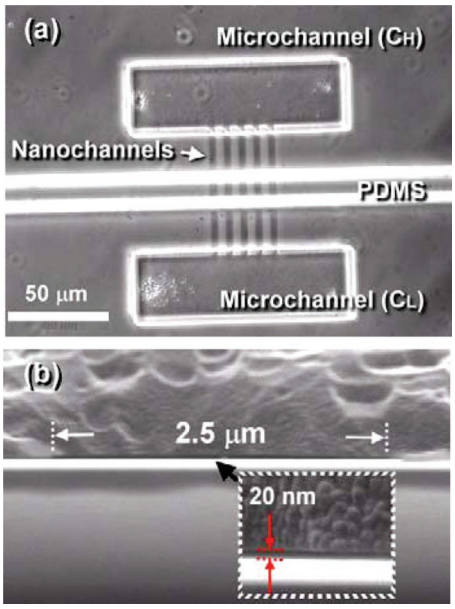

Figure 2. (a) Phase-contrast microscopic top-view image of the device. Five 60 μm long nanochannels connect between two microfluidic channels. The two rectangles are the contact holes connecting the nanochannels and microchannels. The transparent bar lying across the nanochannels is a PDMS wall separating two microchannels. (b) Cross section SEM image shows that each nanochannel is 2.5 μm wide and ~20 nm thick. The bright line in the SEM is the bottom surface extending out of the nanochannel.

scopic images of the device. The 20 nm thick nanochannels were fabricated by removing a 20 nm thick sputtered a-Si sacrificial layer by gaseous XeF_2. The channel thickness, however, can be reduced further if Cr sacrificial layers and a wet-etch process are applied. After etching away the 20 nm-thick Cr sacrificial layer, DI rinsing, and drying the structure, the nanochannels collapsed due to capillary force. Because the e-beam evaporated Cr layer has a relatively rough surface, instead of pinching completely, the nanochannels shrank in the vertical dimension and left a small gap between top and bottom silica surfaces. (see Supporting Information for more details about device fabrication). By measuring the current−voltage ($I-V$) characteristics of the nanochannels and fitting the experimental ion conductance at varied KCl concentrations, the thicknesses of the two nanochannels were extracted to be ca. 18.7 and 4 nm, respectively (see Supporting Information).[11] Their surface charge densities were very close and were about 4.5 mC/m^2 (see Supporting Information). The extracted surface charge density is in the range of the reported data on silica surface[12] but lower than those acquired in the prior works.[6,11,13] The discrepancy may result from the different oxide materials that are produced by different processes. Apart from the surface charge, it is worth emphasizing that the predicted height of the thin channel, 4 nm, is calculated by using the ion mobilities in the bulk.[14] The real ion mobilities can be lower in sub-5 nm geometry due to the fixed charge and the ion proximity to the channel walls.[15] If the reduction of ion mobilities is considered, we should obtain a higher surface charge density as well as a channel height greater than 4 nm.

Three regimes in $I-V$ characteristics were observed when the nanochannel connects to two KCl reservoirs containing solutions of different concentrations: one side with lower concentration was termed C_L and was fixed at 0.1 mM while the other side with high concentration was termed C_H and varied from 0.1 mM to 1 M. The three regimes are symmetric regime (i.e., ohmic behavior), rectifying regime, and weakened rectifying regime. The $I-V$ characteristics corresponding to different C_H and with fixed $C_L = 0.1$ mM are plotted in Figure 3(I.a−e) and 3(II.a−e). The zero-current potentials in the $I-V$ curves were mostly due to the offset electrode potentials, which were produced by the unequal voltage drops at the electrode−electrolyte interface in different electrolyte concentrations (see Supporting Information). The forward-bias conductance, reverse-bias conductance, and the rectifying factor I_F/I_R, are summarized in Figure 3(I.f) and 3(II.f). I_F and I_R were the currents measured at −5 and 5 V, respectively. In the symmetric regime, when C_H is lower than 10 mM (for 4 nm channel) or 1 mM (for 20-nm channel), both I_F and I_R are almost identical and the nanochannels showed the anticipated ohmic behavior in conducting ionic currents. Although the reservoir concentration is asymmetric, the current level is comparable to the results obtained in the case of symmetric concentration (i.e., $C_L = C_H = 0.1$ mM). In the second regime, the current becomes asymmetric with respect to forward and reverse voltage bias. As shown in

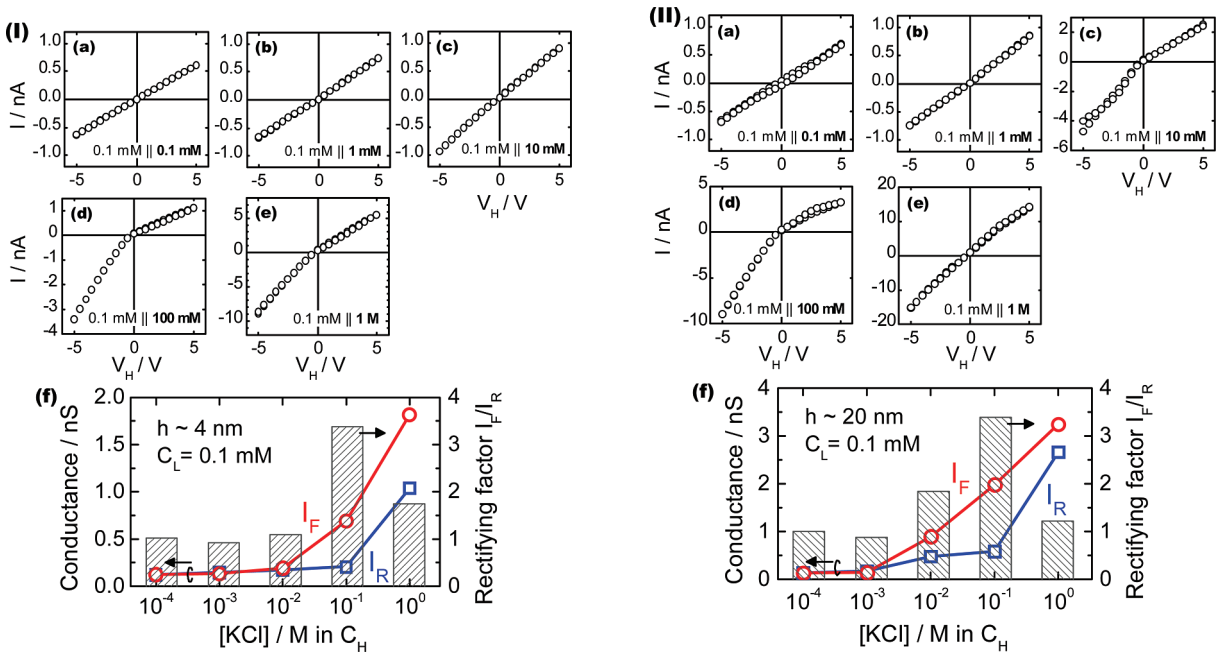

Figure 3. Measured $I-V$ characteristics of 4 nm thick nanochannels (Ia−e) and 20 nm thick nanochannels (IIa−e) under various asymmetric concentrations ($C_L||C_H$). The forward-biased and reverse-biased conductances and the rectifying factor I_F/I_R are summarized in (If) and (IIf) for 4 nm and 20 nm thick nanochannel, respectively. The concentration in left side (C_L) is fixed at 0.1 mM, while the right side (C_H) varies from 0.1 mM to 1 M. The channel width is 2.5 μm × 5 and length 60 μm.

Figure 3(I.f) and 3(II.f), the rectifying effect is maximized at $C_H = 0.1$ M with $I_F/I_R \sim 3.5$. However, in the third regime when the C_H was increased to 1 M, both I_F and I_R increased, yielding weaker asymmetric $I-V$ characteristics. In comparison, the rectifying behavior cannot be observed in microfluidic channels.

The asymmetric ion conduction behaviors under different concentration gradients were qualitatively investigated by calculating the ion distribution profiles in the nanochannel using two-dimensional Poisson-Nernst−Planck (PNP) and continuity equations.[16] Electroneutrality is maintained in the entire system. Because the phenomenon takes place under an applied potential, it represents a nonequilibrium problem. With the channel length much longer than the Debye length, the phenomena cannot be explained with the approximation of constant-field and constant-concentration gradient.[17] The system used for simulation is a 10 μm long, 20 nm thick nanochannel straddled by two 2 μm size square reservoirs. The length of 10 μm, which is shorter than the real device, was used to reduce simulation time. The surface charge density on the channel walls is assumed to be 4.5 mC/m^2, which corresponds to the experimental data. Boundary conditions are set such that the bulk concentration and potential for each reservoir are located 2 μm away from the entrances of the nanochannel. The concentration and potential of the left boundary are fixed to 0.1 mM and 0 V, respectively. More details about the simulation, including the boundary conditions and mesh size used, are described in Supporting Information. The calculated electric potential and profiles of ion concentration averaged across the thickness of the nanochannel are plotted in Figure 4.

At low C_H concentration, i.e., 1 mM at which $\lambda_D \sim$ 10 nm, the EDLs overlap along the entire channel. As a result, the concentration of K ions is enhanced while that of Cl ions suppressed compared with bath concentrations (Figure 4a). When the C_H reservoir is biased, both K and Cl ion concentrations slightly increase but the profiles remain flat in the channel. With such low ion concentrations in both sides, cf. Figure 1a, the EDL (the region inside the dashed boundary) overlap occurs despite the asymmetry in the reservoir concentrations. Because the diffusive fluxes of both K and Cl ions are toward the same direction, resulting in a negligible net diffusion current, we can envisage that the ionic conductance in the nanochannel is mostly contributed by ion drift current driven by the electric field. Thus the amount of ion residing in nanochannel mirrors its conductance. Here, the ion concentrations in the nanochannel are controlled by the surface charge; hence, the applied potentials in the baths have marginal influence on the ion concentration inside the channel although they induce accumulation or depletion of ions near the channel entrance on either side. As a result, either positive or negative bias leads to almost the same ion concentration level and potential gradient, which explains the measured symmetric $I-V$ characteristics. The rectifying factor I_F/I_R acquired from 4 nm and 20 nm thick nanochannels share a similar trend except that the 4 nm channel can maintain symmetric behavior up to 10 mM concentration while the 20 nm channel cannot. This is simply because the Debye length at 10 mM concentration ($\lambda_D \sim 3$ nm) is still larger than half of the channel size, inducing a complete EDL overlap in the 4 nm channel.

As the C_H bath increases to 10 or 100 mM, the ion concentration profile, as shown in Figure 4b,c, either buckles up or slumps depending on the polarities of the applied voltage. At zero bias, ion concentration gradients form along the nanochannel due to diffusion. However, when C_H is

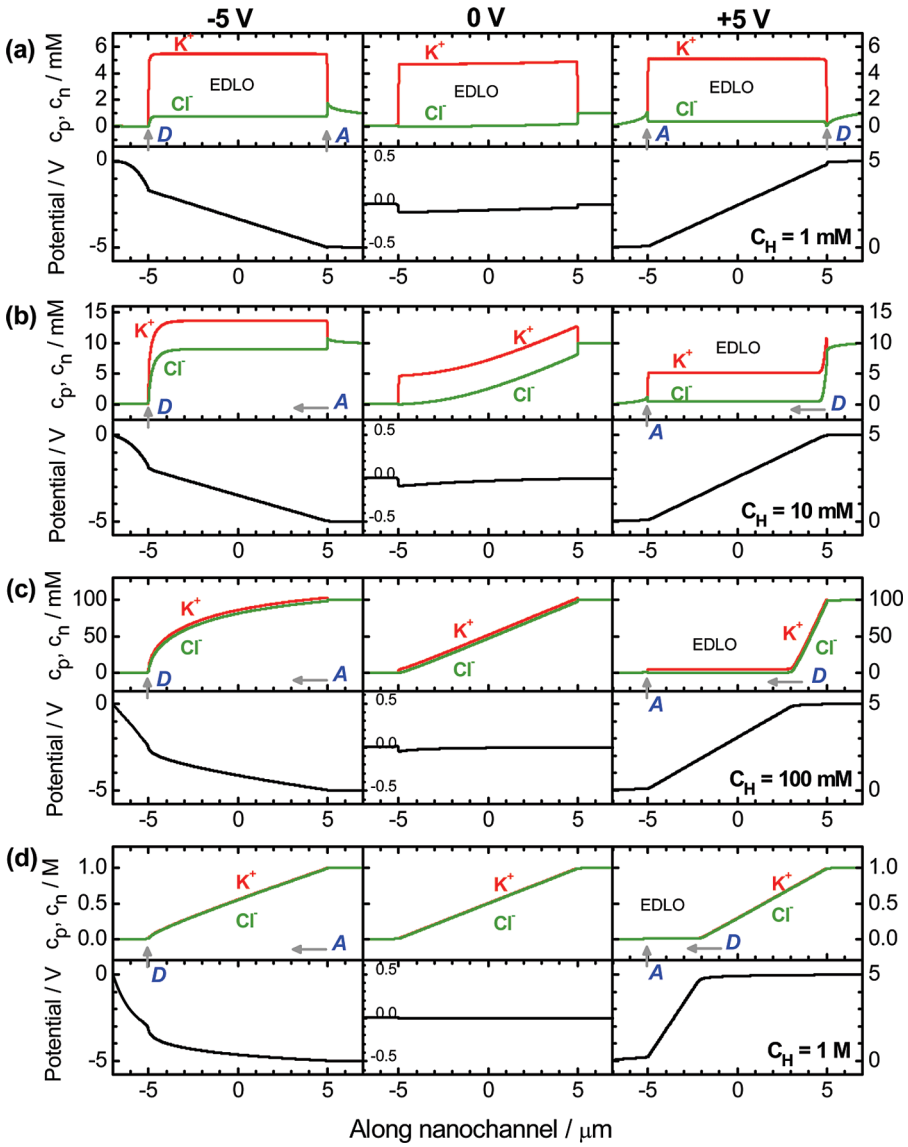

Figure 4. Calculated ion concentration (c_p and c_n) and potential profiles along a 20 nm thick, 10 μm long nanochannel (from $x = -5$ to 5 μm) placed between two KCl reservoirs containing different concentrations C_L (left) and C_H (right). In this system, C_L is set at ground potential and the concentration fixed to 0.1 mM, while C_H is set at (a) 1 mM, (b) 10 mM, (c) 0.1 M, or (d) 1 M and is biased at -5, 0, or 5 V, shown in the columns from left to right. The results represent the averaged values taken across the height of the nanochannel as well as the areas with 20 nm high in the two reservoirs extending laterally from the nanochannel. The potential profiles at zero bias are plotted with an exaggerated scale. EDLO stands for EDL overlap. The *A* or *D* with indications denotes the locations of the accumulation or depletion of ions.

negatively biased, a large amount of K and Cl ions accumulate from the C_H side, leaving upraised concentration gradients in the C_L side. The elevated cation and anion concentrations in the nanochannel lead to high channel conductance. On the other hand, when C_H is positively biased, both cations and anions are depleted to a low concentration resulting in extension of EDL overlap along the nanochannel and hence low channel conductance. It is this different ion distribution that produced the rectifying effect observed in this regime.

With high concentration in C_H, 1 M for example, the amount of ions is large enough to shield the surface charges in nanochannels. In this case, almost no EDL overlap occurs throughout the entire channel except its very left end. As can be seen in Figure 4d, the accumulation or depletion of both K and Cl ions are relatively less manifest and produce a large, constant ion gradient along the channel. The reason for the weakened accumulation when C_H is negative bias is that the potential drop in the nanochannel is alleviated due to the access resistance produced by the depletion of ions around the channel access in the C_L bath. The higher the C_H, the greater the voltage drops across the access resistance in the C_L bath. In this case, the measured conductance is no longer the intrinsic property of the nanochannel. On the other hand, at positive bias, the amount of ion depletion is comparably small as the background ion concentration in the nanochannel increases with high C_H. Voltage biases of different polarities show less influence on ion distribution; therefore, the asymmetric $I-V$ characteristic is not observable.

While the calculated potential and concentration profiles obtained by solving PNP equations account for the asymmetric channel conductance, it brings up an interesting question: why do the ions in nanochannels accumulate or deplete in the response to different bias polarities? The phenomenon can be explained by simply analyzing the drift current of K and Cl ions near the entrances at both sides of the nanochannel at the starting point of the transition right after the voltage is applied and the space charge that causes nonuniform electric potential has built up. In this moment, ionic concentrations are still nearly identical to that at equilibrium state and diffusion fluxes are negligible. Electroneutrality is assumed to be preserved in the transient phase when ionic concentrations change over time and reach steady-state values. This method is an extension of Pu's analysis in explaining a similar effect at the nanochannel−microchannel interface.[18] In their work, the ion-enrichment and ion-depletion effect was observed at low concentration by fluorescent microscopy. The effect also appears in our calculated result by PNP theory in the case of low concentrations shown in Figure 4a at which the EDLs overlap throughout the channel. However, what is interesting is that, when the bath concentration rises on one side, the ion accumulation and depletion develop inside the nanochannel. The resulting enhanced and lessened channel conductance hence becomes observable via electrical measurement.

Referring to Figure 5a, here we consider the average ion concentration of K and Cl ions outside and adjacent to the right entrance of the nanochannel. Because at equilibrium the concentrations of K and Cl ions are considered to be equal in the bath but are unequal in the charged nanochannel, we have the relationship of $[K]_{B,R} = [Cl]_{B,R}$ in the bath and $[K]_{n,R} = \alpha[Cl]_{n,R}$ in the nanochannel, where α is the cation/anion ratio ($\alpha > 1$ for negatively charged nanochannels); B and n in the subscript denote the bath and the nanochannel regions, respectively, while R is the right-hand side. Likewise, a similar relation $[K]_{n,L} = \beta\,[Cl]_{n,L}$ can be set up for the left entrance of the nanochannel. Because the bath concentration on the right side is higher, apparently we can get $\beta > \alpha \geq 1$. In Donnan equilibrium, the cation/anion ratio α can be expressed as $\alpha = (-f + \sqrt{f^2+4c_b^2})^2/4c_b^2$, where c_b and f represent the bulk ion concentration outside and the nanochannel fixed charge concentration, respectively ($f = 2\sigma_s 10^{-3}/qN_A h$, where σ_s, h, and N_A are surface charge density (C/m^2), channel height, and Avogadro's number, respectively).[19] The lower the c_b, or the larger the f, the greater the cation/anion ratio α it builds up. When $c_b > f/2$ (ca. 2.3 mM for $h = 20$ nm and $\sigma_s = 4.5$ mC/m^2 or equivalently $\alpha < 5.83$), the cation/anion ratio decreases as the surface charge has less influence on the ions in nanochannels. It should be notified that the proposed equation for cation/anion ratio is only an approximation for the case of high bath concentration at which nanochannels contain nonuniform potential across the cross section.

When a negative bias is applied to the right C_H side, drift currents are produced due to both K and Cl ions migrating toward the opposite directions. By considering the currentof ion i (i = K or Cl) developed in the nanochannel ($J^i_{n,x}$) and

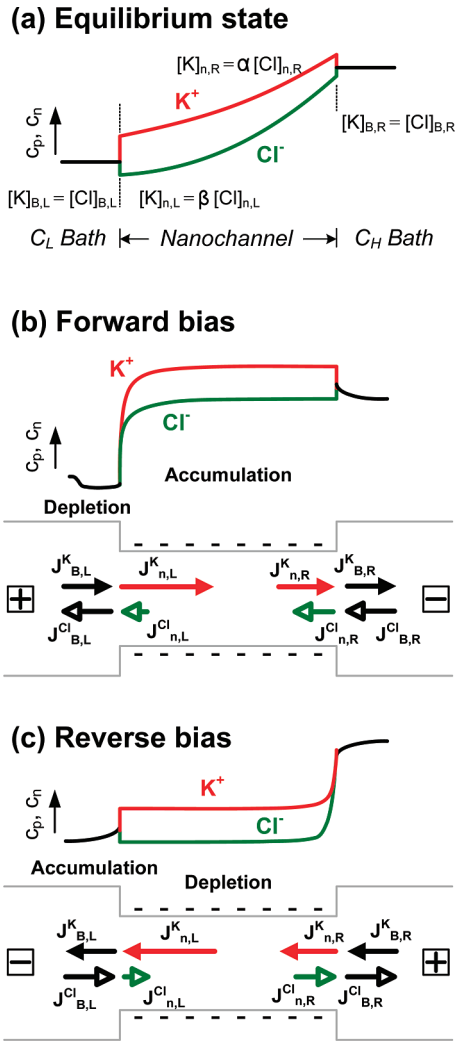

Figure 5. (a) Schematics of the simple model for the interpretation of the ionic rectifying behavior in a charged nanochannel containing concentration gradient. The information of the two bath concentrations are coupled to cation/anion ratios, α and β. (b) When the device is forward biased at which the applied electric field is against the concentration gradient, both K and Cl ions accumulate in the nanochannel and deplete at the channel entrance in C_L bath. (c) When a reverse bias is applied such that the electric filed directs along the concentration gradient, the ions are depleted in the nanochannel and accumulate at the channel entrance in C_L bath. The unbalanced ion currents produced under different bias polarities result in accumulation or depletion of ions in the nanochannel and hence asymmetric channel conductance.

in the bath ($J^i_{B,x}$) on the x side (x = L or R for left or right, respectively) and combining with Kirchoff's current law, we obtain the relations between the drift current in the nanochannel and the bath near the right entrance for K or Cl ions. The current relations are given by[18]

$$J^{K}_{B,R} = \frac{\alpha^{-1} + \mu_K/\mu_{Cl}}{1 + \mu_K/\mu_{Cl}} J^{K}_{n,R}$$

$$J^{Cl}_{B,R} = \frac{1 + \alpha\,\mu_K/\mu_{Cl}}{1 + \mu_K/\mu_{Cl}} J^{Cl}_{n,R} \qquad (1)$$

where the subscripts B and R represents the bath and the right side. By imposing an approximation that the electro-

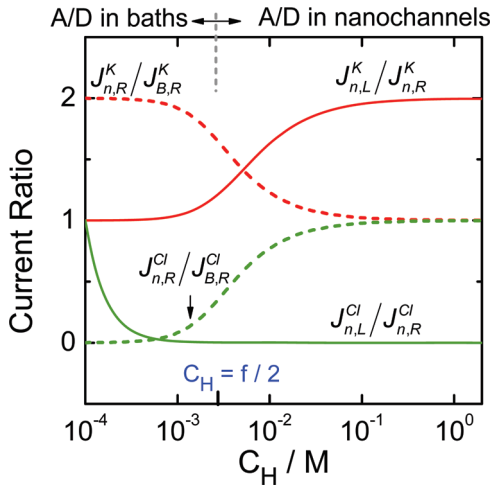

Figure 6. Plot of current ratios vs C_H with $C_L = 10^{-4}$ M. The ratios of the currents developed in the left-hand and right-hand sides of the nanochannel $J_{n,L}/J_{n,R}$ (solid lines) for K and Cl ions approach unity when $C_H < f/2$ but diverge when $C_H > f/2$. The ratios of the currents developed inside and outside the nanochannel $J_{n,R}/J_{B,R}$ (broken lines) for K and Cl ions converge to unity when $C_H > f/2$ but diverge when $C_H < f/2$. The results represent the accumulation−depletion (A/D) of ions takes place in the bath at low C_H but in the nanochannel at high C_H.

phoretic mobilities μ_K and μ_{Cl} are very close,[14] the ratios of the current in the nanochannel to that in the bath for different ions are simplified to:

$$J^{K}_{n,R}/J^{K}_{B,R} = 2/(1 + \alpha^{-1})$$
$$J^{Cl}_{n,R}/J^{Cl}_{B,R} = 2/(1 + \alpha) \qquad (2)$$

Similarly, those near C_L side are $J^{K}_{n,L}/J^{K}_{B,L} = 2/(1 + \beta^{-1})$ and $J^{Cl}_{n,L}/J^{Cl}_{B,L} = 2/(1 + \beta)$. These equations describe the current ratios of single ion species at micro-/nanochannel interfaces. By combining the above equations and the continuity of the total currents inside at the two ends of the nanochannel, the ratios of the ion currents flowing via the left side of the nanochannel to that via the right side are expressed as following

$$\frac{J^{K}_{n,L}}{J^{K}_{n,R}} = \frac{1 + \alpha^{-1}}{1 + \beta^{-1}}$$
$$\frac{J^{Cl}_{n,L}}{J^{Cl}_{n,R}} = \frac{1 + \alpha}{1 + \beta} \qquad (3)$$

For $C_L = 10^{-4}$ M, β is calculated to be ca. 2185. The current ratios in eqs 2 and 3 with respect to C_H are plotted in Figure 6. When $C_H < f/2$, the current ratios $J_{n,L}/J_{n,R}$ for K and Cl ions approximate unity while $J_{n,R}/J_{B,R}$ for K and Cl ions are very different. The resulting relation indicates that $J^{K}_{n,R} > J^{K}_{B,R}$ and $J^{Cl}_{n,R} < J^{Cl}_{B,R}$. In this case, depending on the bias polarity, the accumulation or depletion of both types of ion take place near the channel entrance in the right C_H bath. A similar relation can be obtained in the C_L bath. Because the ion concentration profiles in the nanochannel do not alter with the bias polarity, the ion conductance is symmetric. On the contrary, when $C_H > f/2$, we have $J^{K}_{n,L} > J^{K}_{n,R}$ and $J^{Cl}_{n,L} < J^{Cl}_{n,R}$, while at the right entrance of the channel the ion currents developed inside and outside the nanochannel are very close. As the device is forward biased (Figure 5b), i.e., the applied electric field is opposite to the concentration gradient, more ions are dragged into the channel while less are taken out. These uneven fluxes induce accumulation of both K and Cl ions in the nanochannel and depletion near the channel entrance in C_L bath. Opposite results can be obtained at a reverse bias if the electric field is applied along the concentration gradient. In this condition, as illustrated in Figure 5c, more ions are taken out of the channel than are being injected into the channel, resulting in the depletion of ions in the nanochannel. The results explain why the ion concentration profiles buckle up at $V_H = -5$ V but sinks at $V_H = 5$ V, as shown in Figure 4. In addition to the ion behavior in the nanochannel, the accumulation and depletion of ions at the channel accesses can affect the channel conductance. The depletion of ions, especially at the channel access in the low-concentration C_L bath, increases the resistance of the ion flux and therefore generates an access resistance connecting in series with the nanochannel. When C_H increases to 1 M, the ionic solution with high concentration intrudes deeper from the right bath to the left end of the channel due to diffusion. The channel becomes relatively more conductive than the access resistance in the C_L bath. As a result, the amount of ions to be accumulated or depleted in the nanochannels becomes relatively lower due to the weakened electric field inside the nanochannel. The smaller change of ion concentration in response of applied potential leads to less rectifying effect. Apart from the silica nanochannels, the analysis can also be applied to the nanochannels containing positive surface charge. In that case, we will have the relation of the cation/anion ratios to be $1 > \alpha > \beta > 0$. The rectifying effect will respond to the opposite bias polarity. This result implies that the polarity of surface charge can be probed electrically by measuring the asymmetric $I-V$ characteristics under a concentration gradient besides its reversal potential, which requires Ag/AgCl reference electrodes with saturated KCl bridges.

It is worthwhile to point out that most of the rectifying effects observed in nanofluidic devices or membranes share a similar property of unequal cation/anion ratio or equivalently built-in potential at either entrance (i.e., $\alpha \neq \beta$ or $V_{BI,L} \neq V_{BI,R}$). The cation/anion ratio α and the built-in potential at the channel entrance have the relation of $V_{BI} = kT/2q \ln \alpha$.[20] Here, cation/anion ratio is preferred due to its direct relation to ion currents. A conical nanopore, for example, utilize different pore sizes h, which is equivalent to different fixed charge concentrations f on both sides to achieve the condition $\beta > \alpha \geq 1$. Also, a p−i nanofluidic diode[9] with negative and neutral surface charges in the two sides of the nanochannel has the condition of $\beta > \alpha = 1$; while a p−n nanofluidic diode (negative−positive surface charge)[10] or a bipolar membrane has $\beta > 1 > \alpha > 0$. All of these devices take advantage of asymmetric geometry or surface charge

rather than different concentrations to produce asymmetric cation/anion ratio. Apart from the physical asymmetry of the nanochannels, based on the discussion above, the bath concentrations should nevertheless be sufficiently high to eliminate the access resistance generated by the depletion of ions in the baths of low concentrations, which was also observed in the characterization of nanofluidic diodes,[9] and produce the accumulation or the depletion of ions inside the nanochannels to maximize rectifying effect.

In conclusion, the ionic rectifying effect was experimentally and theoretically investigated in 4 and 20 nm thick silica nanochannels under various concentration gradients. When the bath concentrations were set up to induce EDL overlap at the single side of the nanochannel, the rectifying effect appears. On the basis of the calculated ion profiles and the simplified model, we attribute the phenomenon to the accumulation or depletion of both cations and anions in nanochannels in response to different bias polarities. The model indicates that the basis of the ionic rectifying effect in the nanofluidic devices reported so far is to produce asymmetric cation/anion ratios or built-in potentials at the two entrances of the nanochannels. The condition, therefore, allows the accumulation and depletion of ions in nanochannels to be controllable by applied potential. The analysis also interprets the electrokinetic behavior at the junction of nanochannels and baths at low ionic concentrations. The result implies that the physics of nanofluidics may not be singled out without considering the nanofluidic−microfluidic interface. The study improved our understanding of electrokinetic ion transport through nanochannels and will benefit the design of nanofluidic devices for attoliter to zeptoliter-scale chemical delivery.

Acknowledgment. This work was supported by a Riethmiller Fellowship and the National Science Foundation (ECS-0424204).

Supporting Information Available: Device fabrication, measurement, zero-current potentials in asymmetric ion concentration, simulation. This material is available free of charge via the Internet at http://pubs.acs.org.

References

(1) Kasianowicz, J. J.; Brandin, E.; Branton, D.; Deamer, D. W. *Proc. Natl. Acad. Sci. U.S.A.* **1996**, *93*, 13770−13773.
(2) Kuo, T. C.; Cannon, D. M.; Chen, Y. N.; Tulock, J. J.; Shannon, M. A.; Sweedler, J. V.; Bohn, P. W. *Anal. Chem.* **2003**, *75*, 1861−1867.
(3) Karnik, R.; Castelino, K.; Fan, R.; Yang, P.; Majumdar, A. *Nano Lett.* **2005**, *5*, 1638−1642.
(4) Dekker, C. *Nat. Nanotechnol.* **2007**, *2*, 209−215.
(5) Israelachvili J. *Intermolecular and Surface Forces*, 2nd ed; Academic Press: London, 2003. For 1:1 electrolyte solutions, $\lambda_D \sim 0.307/\sqrt{c_b}$ at room temperature, where c_b is bath concentration.
(6) Stein, D.; Kruithof, M.; Dekker, C. *Phys. Rev. Lett.* **2004**, *93*, 4.
(7) Kovarik, M. L.; Jacobson, S. C. *Anal. Chem.* **2007**, *79*, 1655−1660.
(8) Siwy, Z. S. *Adv. Funct. Mater*. **2006**, *16*, 735−746.
(9) Karnik, R.; Duan, C. H.; Castelino, K.; Daiguji, H.; Majumdar, A. *Nano Lett.* **2007**, *7*, 547−551.
(10) Vlassiouk, I.; Siwy, Z. S. *Nano Lett.* **2007**, *7*, 552−556.
(11) Schoch, R. B.; Renaud, P. *Appl. Phys. Lett.* **2005**, *86*, 3.
(12) Behrens, S. H.; Grier, D. G. *J. Chem. Phys.* **2001**, *115*, 6716−6721.
(13) Karnik, R.; Fan, R.; Yue, M.; Li, D. Y.; Yang, P. D.; Majumdar, A. *Nano Lett.* **2005**, *5*, 943−948.
(14) The ion mobilities: $\mu_K = 7.619 \times 10^{-8}$ m^2/V s, $\mu_{Cl} = 7.912 \times 10^{-8}$ m^2/V s.
(15) Ho, C.; Qiao, R.; Heng, J. B.; Chatterjee, A.; Timp, R. J.; Aluru, N. R.; Timp, G. *Proc. Natl. Acad. Sci. U.S.A.* **2005**, *102*, 10445−10450.
(16) Eisenberg, R. S. *J. Membr. Biol.* **1999**, *171*, 1−24.
(17) Chen, D. P.; Barcilon, V.; Eisenberg, R. S. *Biophys. J.* **1992**, *61*, 1372−1393.
(18) Pu, Q. S.; Yun, J. S.; Temkin, H.; Liu, S. R. *Nano Lett.* **2004**, *4*, 1099−1103.
(19) Lakshminarayanaiah N. *Equations of Membrane Biophysics*; Academic Press: New York, 1984. In Donnan equilibrium, the averaged cation concentration and anion concentration are given by $\bar{c}_+ = -f/2 + \sqrt{(f/2)^2+c_b^2}$ and $\bar{c}_- = f/2 + \sqrt{(f/2)^2+c_b^2}$, respectively. The sign of f depends on the polarity of the fixed surface charge in the nanochannels.
(20) $V_{BI} = kT/q \ln(f/2c_b + \sqrt{(f/2c_b)^2+1})$ or $V_{BI} = kT/2q \ln \alpha$. The equation is valid for low c_b but is an approximation for high c_b ($c_b \gg f/2$).

NL071770C